Manipulation of band electrons with a rectangular-wave electric field

1999 J. Phys.: Condens. Matter 11 4527

(http://iopscience.iop.org/0953-8984/11/23/307)

J. Phys.: Condens. Matter **11** (1999) 4527–4538. Printed in the UK PII: S0953-8984(99)02975-6

Manipulation of band electrons with a rectangular-wave electric field

Ming Jun Zhu†, Xian-Geng Zhao†‡ and Qian Niu§

† Institute of Applied Physics and Computational Mathematics, PO Box 8009, Beijing 100080, People's Republic of China

‡ Institute of Theoretical Physics, Academia Sinica, PO Box 2735, Beijing 100080, People's Republic of China

§ Department of Physics, The University of Texas at Austin, Austin, TX 78712-1081, USA

Received 24 March 1999

Abstract. We study the propagation of an electron in a superlattice under the action of a rectangular-wave electric field. Exact results for any initial distribution and long-range hopping couplings are obtained. Total collapse of the quasi-energy spectrum is found to take place at suitably chosen field parameters, which leads to the transition between localization and delocalization. Moreover, this localization/delocalization behaviour persists even if long-range hoppings are taken into account. The transport property of the system is also investigated where the signatures of the transition between localization and delocalization as well as fractional Wannier–Stark ladders are manifested.

1. Introduction

Work on manipulating evolution behaviour of band electrons with external electric fields has progressed considerably in recent years. Much interest has been focused on the propagation of electrons in spatially periodic structures driven by time-dependent electric fields [1–4]. One principal idea that emerged from the studies is that the dynamic properties of electrons are tunable through adjustment of the external-field parameters, such as amplitude and frequency, with real experimental consequences.

Since the 1960s it has been known that a uniform electric field can destroy the Bloch band structure of a crystal lattice, resulting in the so-called Wannier–Stark ladders [5]. The experimental confirmation of this effect has been established by optical absorption spectra measurements on semiconductor superlattices [6], and more recently for a system of ultra-cold atoms in an accelerating optical potential [7–9]. The evolution of electrons driven by an ac field was also studied in great detail, and the phenomenon of dynamic localization is found to occur when the field parameters of the driving field are set at certain values [10, 11]. This effect has been observed in a recent experiment by the use of free-electron lasers [12], where the absolute negative conductance in the I–V characteristics is recognized as a signature of the dynamic localization.

To be precise, total band collapse under an ac electric field can be achieved only in the nearest-neighbour coupling approximation [13]. There are some practical systems in which couplings beyond the nearest neighbours are important [14]. Also, new and fascinating effects have been predicted in the general situation for a system driven by a combined ac–dc electric field [13]. The result depends critically on the matching ratio of the Bloch frequency and the ac frequency [15]. If the ratio is irrational (but not a Liouville number) [16], the energy spectrum is a discrete point structure with all of the states localized [13]. If the ratio is rational, the energy spectrum forms a fractional Wannier–Stark ladder [17] with extended energy states. The bandwidth is mainly given by the qth-neighbour coupling constant times the pth-order Bessel function, where p/q is the rational fraction in irreducible form. The Bessel function has its argument proportional to the relative strength of the ac and dc electric fields, and can thus be tuned to collapse the bandwidth. The collapse can only be achieved approximately, however, if the remainder of the contributions to the bandwidth from couplings between multiple qth neighbours are taken into account.

In the above discussions, the ac field is assumed to be a sinusoidal function of time. In this work, we investigate the effects of a different kind of time-periodic electric field, i.e., a rectangular-wave field. We will find that the approximate band collapse for systems with couplings beyond nearest neighbours can be made exact with rectangular-wave fields. The field has the characteristic that it is constant with an alternating sign change within the period. In the first period it is given by

$$F(t) = \begin{cases} F & 0 \leqslant t < \alpha T/2 \\ -F & \alpha T/2 \leqslant t < T - \alpha T/2 \\ F & T - \alpha T/2 \leqslant t < T \end{cases} \tag{1}$$

where F is the field magnitude, T the period length, and $0 < \alpha < 1$. When α is not equal to $1/2$, the field will have both a dc and an ac component. A Bloch electron may undergo either localized or delocalized motion, depending upon the value of the matching ratio T/T_0, where T_0 is the Bloch period for the dc component [18], as well as the value of α. When the matching ratio is irrational, localization takes place regardless of the choice of α. It will be shown that when the matching ratio equals an integer or a rational number, the motion will be delocalized except for certain values of α where band collapse and dynamical localization take place. More importantly, unlike in the case where the ac component of the field is a sinusoidal function of time, this phenomenon of localization/delocalization transition can, for the appropriate choice of α, hold rigorously even if the long-range hopping couplings are involved. Therefore, it should be more easily observed experimentally.

The rest of this work is laid out as follows. In section 2, we will present detailed analytical results for the amplitude propagators, the field-induced polarization, and the mean square displacement, from which the localization conditions will be deduced. In section 3 we obtain the quasi-energy spectrum and the current–voltage characteristic curve. There it is found that the suppression of the quasi-energy band coincides with the onset of the coherent destruction of the tunnelling. Finally, a brief summary with discussion will be given in section 4.

2. Amplitude propagators, polarization, and mean square displacement

For the sake of simplicity, we consider an electron with charge e moving in a one-dimensional long-period superlattice of period a driven by the field $F(t)$. The field is along the growth axis $\boldsymbol{x}$ of the superlattice, resulting in the time-dependent potential $eF(t)x$, in addition to the periodic lattice potential $V(x) = V(x + a)$. From the dynamical point of view, the process of Zener tunnelling is sufficiently slow to be considered unimportant [11]. Therefore, we only pay attention to the single-band case. The wave function $\psi(x, t)$ can be expanded as

$$\psi(x, t) = \sum_n C_n(t) \exp(-\mathrm{i}n\theta(t))\phi(x - na)$$

where $\phi(x-na)$ is the Wannier function at the nth well, and $\theta(t)$ is the reduced vector potential defined by

$$\theta(t) = ea\int_0^t \mathrm{d}t'\ F(t'). \tag{2}$$

The amplitude propagators $C_n(t)$ satisfy the following evolution equation [13]:

$$\mathrm{i}\,\frac{\mathrm{d}}{\mathrm{d}t}C_n(t) = \sum_m R_m \mathrm{e}^{-\mathrm{i}m\theta(t)}C_{m+n}(t) \tag{3}$$

where

$$R_m = \int \mathrm{d}x\ \phi^*(x)\Big(-\frac{1}{2\mu}\,\frac{\partial^2}{\partial x^2} + V(x)\Big)\phi(x-ma)$$

and μ is the effective mass of the electron. The solution of equation (3) is given by

$$C_n(t) = \sum_l C_l(0)\int_0^{2\pi}\frac{\mathrm{d}k}{2\pi}\ \exp\mathrm{i}\Big\{(n-l)k - \sum_m R_m\xi_m(t)\cos\left[mk+\alpha_m(t)\right]\Big\} \tag{4}$$

where

$$\xi_m(t) = \left|\int_0^t \mathrm{d}t'\ \mathrm{e}^{-\mathrm{i}m\theta(t')}\right|$$

and

$$\alpha_m(t) = \arg\bigg(\int_0^t \mathrm{d}t'\ \mathrm{e}^{-\mathrm{i}m\theta(t')}\bigg).$$

The field-induced polarization $\langle\Delta x\rangle$ and the mean square displacement $\langle\Delta x^2\rangle$ are defined as

$$\langle\Delta x\rangle(t) = \langle\psi(x,t)|x|\psi(x,t)\rangle - \langle\psi(x,0)|x|\psi(x,0)\rangle \tag{5}$$

$$\langle\Delta x^2\rangle(t) = \langle\psi(x,t)|x^2|\psi(x,t)\rangle - \langle\psi(x,0)|x^2|\psi(x,0)\rangle. \tag{6}$$

After somewhat lengthy but straightforward algebra, by the use of the above expressions, we arrive at

$$\langle\Delta x\rangle(t) = a\sum_l C_l^*(0)U_l(t) \tag{7}$$

$$\langle\Delta x^2\rangle(t) = a^2\sum_l |U_l(t)|^2 - 2a\langle\Delta x\rangle(t) \tag{8}$$

where

$$U_l(t) = \mathrm{i}\sum_m C_{l+m}(0)mR_m\int_0^t \mathrm{d}t'\ \mathrm{e}^{-\mathrm{i}m\theta(t')}. \tag{9}$$

Since the driving field $F(t)$ is periodic in time: $F(t) = F(t+T)$, we find from equations (1) and (2) that $\theta(t+qT) = \theta(t) + q\theta(T), q = 1, 2, \ldots,$ and $\theta(T) = eaFT(2\alpha-1)$. As $2\pi/eaF(2\alpha-1)$ is the Bloch period T_0, the electric matching ratio is just $T/T_0 = \theta(T)/2\pi$.

As can be seen from equations (7) and (8), the quantity $U_l(t)$ plays a central role in our problem. It signifies the tunnelling behaviour of the electron and will serve as a vehicle for us to find the conditions at which the motion of the electron becomes localized. Using equation (9), we obtain

$$U_l(t+qT) = U_l(qT) + \mathrm{i}\sum_m C_{l+m}(0)mR_m\mathrm{e}^{-\mathrm{i}mq\theta(T)}\int_0^t \mathrm{d}t'\ \mathrm{e}^{-\mathrm{i}m\theta(t')} \tag{10}$$

where

$$U_l(qT) = \mathrm{i}\sum_m C_{l+m}(0) m R_m \frac{\mathrm{e}^{-\mathrm{i}qm\theta(T)} - 1}{\mathrm{e}^{-\mathrm{i}m\theta(T)} - 1} \int_0^T \mathrm{d}t'\, \mathrm{e}^{-\mathrm{i}m\theta(t')}. \tag{11}$$

The above results are valid for arbitrary value of the electric matching ratio $\theta(T)/2\pi$. In the following discussion, we will show that the dynamic behaviour of the system can be classified by the number-theoretical properties of the ratio.

2.1. *Rational matching ratio*

If $\theta(T)/2\pi = p/q$, where p and q are relatively prime integers (the integer matching ratio can be viewed as a special case for $q = 1$), one can see from equations (10) and (11) that

$$U_l(t + qT) = U_l(t) + qU_l(T) \tag{12}$$

and if in addition α and F are chosen such that

$$qeaFT\alpha = 2\pi\nu \qquad (\nu = \pm 1, \pm 2, \ldots) \tag{13}$$

every term in $U_l(qT)$ will vanish. Consequently, $U_l(t)$ becomes a temporally periodic function with period qT: $U_l(t + qT) = U_l(t)$. This gives rise to both $\langle \Delta x\rangle(t)$ and $\langle \Delta x^2\rangle(t)$ being bounded and temporally periodic with the same period qT, i.e.,

$$\langle \Delta x\rangle(t + qT) = \langle \Delta x\rangle(t)$$

$$\langle \Delta x^2\rangle(t + qT) = \langle \Delta x^2\rangle(t).$$

This means that at any given time, the electron cannot go far from its initial distribution $C_l(0)$, but instead will maintain an oscillatory and bounded motion around the initial distribution throughout the whole process. This is just the phenomenon of dynamic localization.

Combining the matching ratio and the localization condition (13), α can be expressed in terms of the pair of integers p and ν as $\alpha = \nu/(2\nu - p)$, with the restriction that $p/\nu < 1$. In figure 1(a) we show an example of $U_l(t)$ that satisfies the localization condition (13) with $q = 1$, $\nu = -1$ and $p = 2$ such that $\alpha = 1/4$ and $\theta(T) = 4\pi$. For simplicity and definiteness, only the absolute value of $U_l(t)$ is plotted and we have taken the initial distribution to be $C_{l+m}(0) = \delta_{l+m,0}$. Figure 1(b) displays an example of the rational-matching-ratio case for $p = 2$, $q = 3$, and $\nu = -1$. From these two plots, we can clearly see that the localized evolution is with period qT in the time domain.

In the case where the condition (13) is not met, $U_l(qT)$ is no longer zero, and because of equation (12), $U_l(t)$ will not be periodic. Likewise, the field-induced polarization $\langle \Delta x\rangle(t)$ and the mean square displacement $\langle \Delta x^2\rangle(t)$ are no longer periodic. In fact, it can be shown that

$$\langle \Delta x\rangle(t \to \infty) \to \infty \qquad \langle \Delta x^2\rangle(t \to \infty) \to \infty$$

indicating that the electron will deviate from its initial distribution as time evolves and never return, which of course means delocalization. This is depicted in figure 1(c) for $q = 1$, $p = 2$, and $\alpha = 1/5$.

2.2. *Irrational matching ratio*

If $\theta(T) = 2\pi\gamma$, where γ is irrational, by the number-theoretical technique of reference [15], it can be shown that $U_l(t)$ will always be localized quasi-periodically irrespective of the value of α. Interested readers may consult that paper for more details and here we will only show a picture to illustrate this case in figure 1(d) for $\gamma = \sqrt{7}$ and $\alpha = 1/\sqrt{2}$.

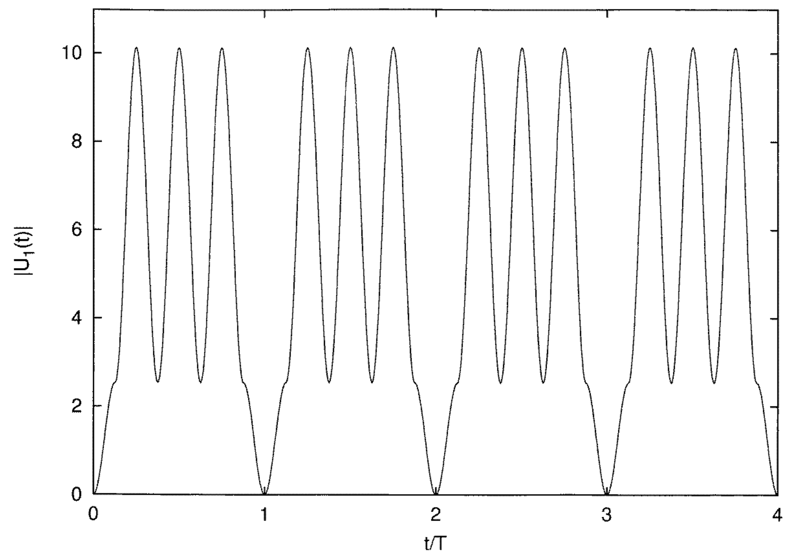

(a)

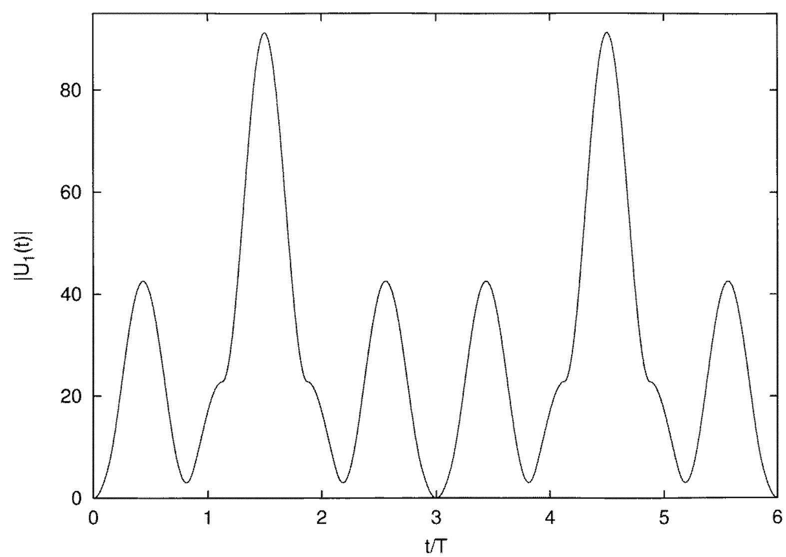

(b)

Figure 1. $|U_l(t)|$ as functions of t/T. The vertical axis is in arbitrary units. (a) $\theta(T)/2\pi = 2$ and $eaFT\alpha/2\pi = -1$; (b) $\theta(T)/2\pi = 2/3$ and $eaFT\alpha/2\pi = -1/3$; (c) $\theta(T)/2\pi = 2$ and $\alpha = 1/5$; (d) $\theta(T)/2\pi = \sqrt{7}$ and $\alpha = 1/\sqrt{2}$.

The above analyses show clearly that the coherent motion of the electron can be coerced into different behaviours by the driving rectangular-wave field through the adjustment of its parameters. The electron may start out in an extended motion in the lattice through quantum tunnelling, but as soon as the field parameters are such that they satisfy one set of the localization conditions, the tunnelling will be destroyed, and the motion localized thereafter. This scenario is consistent with the suppression of the quasi-energy spectrum, which will be presented in the next section.

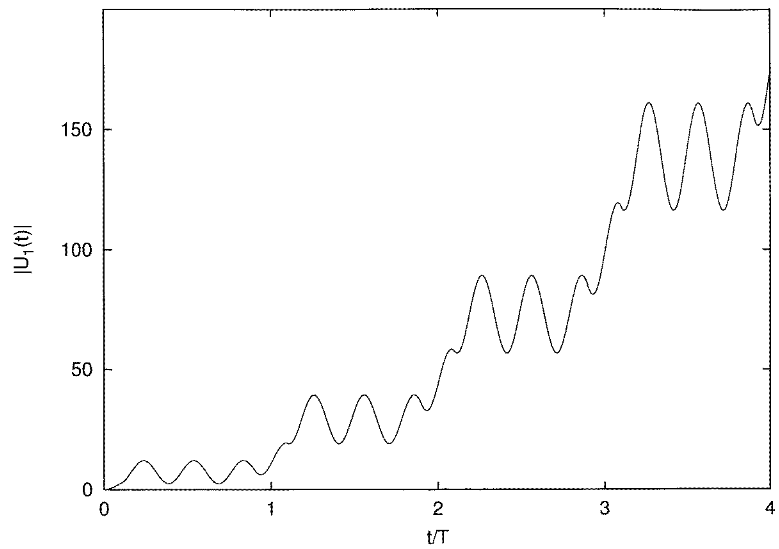

(c)

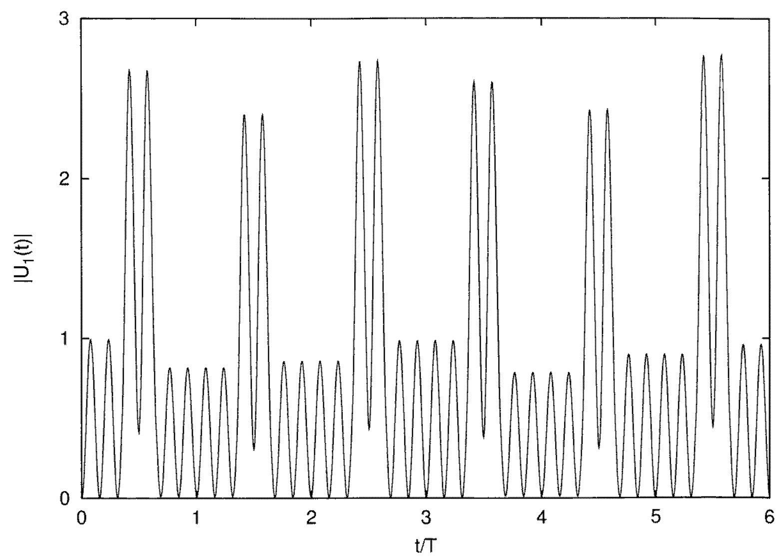

(d)

Figure 1. (Continued)

3. The quasi-energy spectrum and I–V characteristics

The above dynamics of the system will be transparent if we transfer the problem into energy space. Because of the periodicity of the electric field $F(t)$ (with period T), we have the time-periodic electrical potential $eF(t)x$ (with the same period T). Therefore, we can employ Floquet's theorem to write the wave function $\psi(x, t)$ as $\psi(x, t) = \mathrm{e}^{-\mathrm{i}\epsilon t} u_\epsilon(x, t)$, where ϵ is called quasi-energy, and $u_\epsilon(x, t)$ is the time-periodic Floquet function $u_\epsilon(x, t) = u_\epsilon(x, t + T)$. As argued in section 2, when neglecting Zener tunnelling, we can expand $u_\epsilon(x, t)$ by the use of one-band Wannier functions $\phi(x-na)$ associated with the nth well:

$$u_\epsilon(x,t)=\sum_n u_{\epsilon n}(t)\phi(x-na).$$

The coefficients $u_{\epsilon n}(t)$ are periodic in time and satisfy the evolution equations

$$\mathrm{i}\,\frac{\mathrm{d}}{\mathrm{d}t}u_{\epsilon n}(t)=\sum_m R_m u_{\epsilon(m+n)}(t)-[\epsilon-neaF(t)]u_{\epsilon n}(t). \tag{14}$$

On introducing $u_{\epsilon n}(t)=\mathrm{e}^{\mathrm{i}(\epsilon t-n\theta(t))}C_n(t)$, equation (14) reduces to equation (3), whose solution in momentum space k, when employing the discrete Fourier transform

$$C(k,t)=\sum_n C_n(t)\mathrm{e}^{-\mathrm{i}nk} \qquad (-\pi\leqslant k<\pi)$$

is given by

$$C(k,t)=C(k,0)\exp\left(-\mathrm{i}\int_0^t \mathrm{d}t'\ R(\theta(t')-k)\right) \tag{15}$$

where

$$R(\theta(t)-k)=\sum_n R_n\mathrm{e}^{-\mathrm{i}n(\theta(t)-k)}.$$

The periodicity of $u_{\epsilon n}(t)$ means that

$$C_n(T)=C_n(0)\mathrm{e}^{-\mathrm{i}(\epsilon T-n\theta(T))} \tag{16}$$

whose Fourier transform leads to

$$C(k,T)=C(k-\theta(T),0)\mathrm{e}^{-\mathrm{i}\epsilon T}.$$

Substituting this relation into equation (15) yields the eigenvalue equation

$$C(k-\theta(T),0)\mathrm{e}^{-\mathrm{i}\epsilon T}=C(k,0)\exp\left(-\mathrm{i}\int_0^T \mathrm{d}t\ R(\theta(t)-k)\right). \tag{17}$$

The quasi-energy ϵ stems from the condition that nonzero solutions for the coefficients C exist. When $\theta(T)/2\pi$ is an integer, we have

$$\epsilon(k)=\frac{1}{T}\int_0^T \mathrm{d}t\ R(\theta(t)-k) \tag{18}$$

whose dispersion is controlled by the electric field, and will collapse to a constant under the condition $eaFT\alpha=2\pi\nu$ ($\nu=\pm1,\pm2,\ldots$).

When $\theta(T)/2\pi=p/q$ with p and q being relatively prime integers, k is no longer a good quantum number. However, if we write the wavenumber in the form $k=s+2\pi l/q$, where $-\pi/q\leqslant s<\pi/q$ and l is an integer, then s is conserved and we can use it to label the quasi-energy states. Substituting $k=s+2\pi l/q$ into both sides of equation (17), and taking a product on each side over $l=0,1,\ldots,q-1$, we obtain

$$\prod_{l=0}^{q-1}C\left(s+2\pi\frac{l-p}{q},0\right)\mathrm{e}^{-\mathrm{i}q\epsilon T}$$
$$=\prod_{l=0}^{q-1}C\left(s+2\pi\frac{l}{q},0\right)\exp\left(-\mathrm{i}\int_0^T \mathrm{d}t\ \sum_{l=0}^{q-1}R\left(\theta(t)-s-2\pi\frac{l}{q}\right)\right). \tag{19}$$

Since the coefficients C in the product all have the same absolute value according to equation (17), a nontrivial solution to equation (17) should correspond to a nonzero product of the coefficients C on each side of equation (19). Obviously, the products of the coefficients C on the two sides are equal, because $C(k, 0)$ is periodic with period 2π and the set $\{0, 1, \ldots, q-1\}$ is same as $\{-p, 1-p, \ldots, q-1-p\}$ (mod q). Therefore, the exponentials on the two sides of equation (19) must be equal, and we have the quasi-energies

$$\epsilon(n, s) = \frac{1}{qT}\int_0^T \mathrm{d}t \sum_{l=0}^{q-1} R\left(\theta(t) - s - 2\pi\frac{l}{q}\right) + \frac{2\pi n}{qT} \tag{20}$$

where n is an integer which takes values $0, 1, \ldots, q-1$ because the quasi-energy is defined within a Brillouin zone of width $2\pi/T$. Carrying out the summation in equation (20), we obtain the quasi-energy spectrum as

$$\epsilon(n, s) = \sum_j R_{qj}\frac{(1 - \mathrm{e}^{-\mathrm{i}qjeaFT\alpha})}{\mathrm{i}qjeaFT/2}\mathrm{e}^{\mathrm{i}qj(s+eaFT\alpha/2)} + \frac{2\pi n}{qT} \qquad -\frac{\pi}{q} \leqslant s < \frac{\pi}{q}. \tag{21}$$

In general, the quasi-energy $\epsilon(n, s)$ forms band structures with finite widths. However, the bandwidths will vanish entirely if the localization condition equation (13) is adopted in the expression above. This suppression of the quasi-energy band then coincides with the onset of the destruction of the tunnelling discussed earlier. Furthermore, a closer examination of equation (21) reveals a remarkable result: for any integer n not equal to 1, if α is a rational fraction number given by $\alpha = n/(2n-1)$, the bandwidths will collapse for any initial distribution and any range (tight-binding or long-distance) hopping couplings *regardless the value of the electric matching ratio.* This is a much stronger result than any heretofore studied case. In figure 2 we have plotted the quasi-energies versus the matching ratio for the rational case when $eaFT/2\pi = \sqrt{3}$. To mimic their tight-binding nature, the R_{qj} are approximated by an exponential function $\Delta\mathrm{e}^{-|qj|/Q}$, where Δ and Q are lattice-related constants. The value of Q reflects the degree of the strength of the long-range interaction. The quasi-energy is scaled by π/T, which extends over two Brillouin zones $[-2\pi/T, 2\pi/T]$. The matching ratio labels the vertical axis, along which the actual physical quantity being varied is the parameter α. Because of the exponential decay of the hopping matrix element with distance, we have retained only $j = \pm 1$ terms in the summation of equation (21) for this plot.

Because the quasi-energy is taken over two Brillouin zones, for a given rational p/q there will be $2q-1$ subbands, since the two subbands centred at zero overlap. As we can clearly see, these subbands have finite bandwidths, at least for the simple fractions of the matching ratio. Another remarkable feature that the figure shows is its recursive structure of self-similarity. This characteristic is somewhat like that of Hofstadter's 'butterfly' spectrum [19], which involves a Bloch electron in a 2D lattice under the action of a constant magnetic field. That fact suggests to us there may be a congruence between the 2D magnetic problem and the 1D electric problem [15, 17, 20].

Figure 3 shows the case of the total collapse of the quasi-energy bands. The quasi-energy is still scaled by π/T and extends over two Brillouin zones $[-2\pi/T, 2\pi/T]$. To generate this figure, we have taken $eaFT/2\pi = 7p/q$, or equivalently $\alpha = 4/7$. Other parameters are arbitrary. Please note that for any value of $\alpha = n/(2n-1)$, we will reach a picture identical to figure 3, because all of the bandwidths of the quasi-energy subbands will shrink to zero in that case.

The transition between localization and delocalization is also manifested in the transport properties of the system, such as its I–V characteristics. At zero absolute temperature and assuming that the electrons are initially concentrated near the bottom of the band, the averaged dc current is given by [14]

$$J = \frac{\langle j(t)\rangle}{j_0} = \sum_n n\frac{G_n}{G_1}\lim_{T_L\to\infty}\frac{1}{T_L}\int_0^{T_L}\mathrm{d}t \int_0^t \frac{\mathrm{d}t'}{\tau}\,\mathrm{e}^{-(t-t')/\tau}\sin n[\theta(t) - \theta(t')] \tag{22}$$

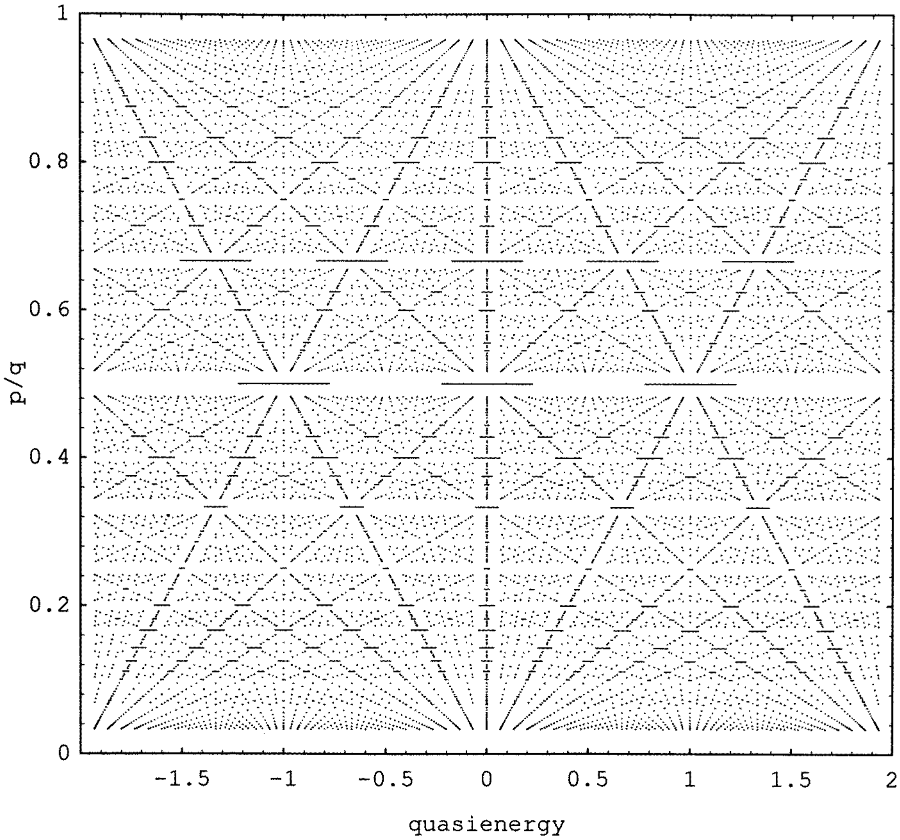

Figure 2. The quasi-energy versus the rational matching ratio p/q, when $2\alpha - 1 = p/q\sqrt{3}$. The energies are drawn over two Brillouin zones and are in units of π/T. Other parameters are $\pi eaF/4\Delta = 2$ and $Q = 5$. Only rationals satisfying $0 < p, q < 30$ are shown.

where the G_n are the Fourier coefficients of the energy band and τ is the relaxation time. We consider a practical model of superlattices with GaAs wells of width 40 Å separated by $Al_xGa_{1-x}As$ barriers of thickness 10 Å. This model gives $G_2/G_1 = -0.202$ and $G_3/G_1 = 0.069$ if we take $x = 0.3$ and the barrier potential as 0.3 eV [14]. The higher-order coefficients can be neglected because of their small magnitudes.

In figure 4 we plot J as a function of the electric matching ratio $\theta(T)/2\pi$ which is proportional to the applied voltage. Here only the nearest-neighbour approximation is used in our calculation. When $\alpha = 6/7$, in addition to the Esaki–Tsu peak [21], there are several peaks at $\theta(T)/2\pi = 1$, 2, and 3. They are the resonant structures of the interplay between the Bloch frequency and the field frequency. As α changes to 3/4 which corresponds to $\nu = 3$ and $p = 2$, the peak at $\theta(T)/2\pi = 2$ disappears (the value of ν is irrelevant here as long as $\nu/p \neq$ integer). When α reaches one of its total-collapse values, $\alpha = 4/7$, all peaks are eliminated except the Esaki–Tsu one.

Figure 5 shows the case of long-range hopping couplings. The upper and lower curves correspond to $\alpha = 6/7$ and $4/7$, respectively. As we can see from the upper curve, besides the resonant peaks at integer values of $\theta(T)/2\pi$, additional features have emerged at $\theta(T)/2\pi = 1/3, 1/2, 2/3$, and 3/2. They are obviously the signatures of fractional Wannier–

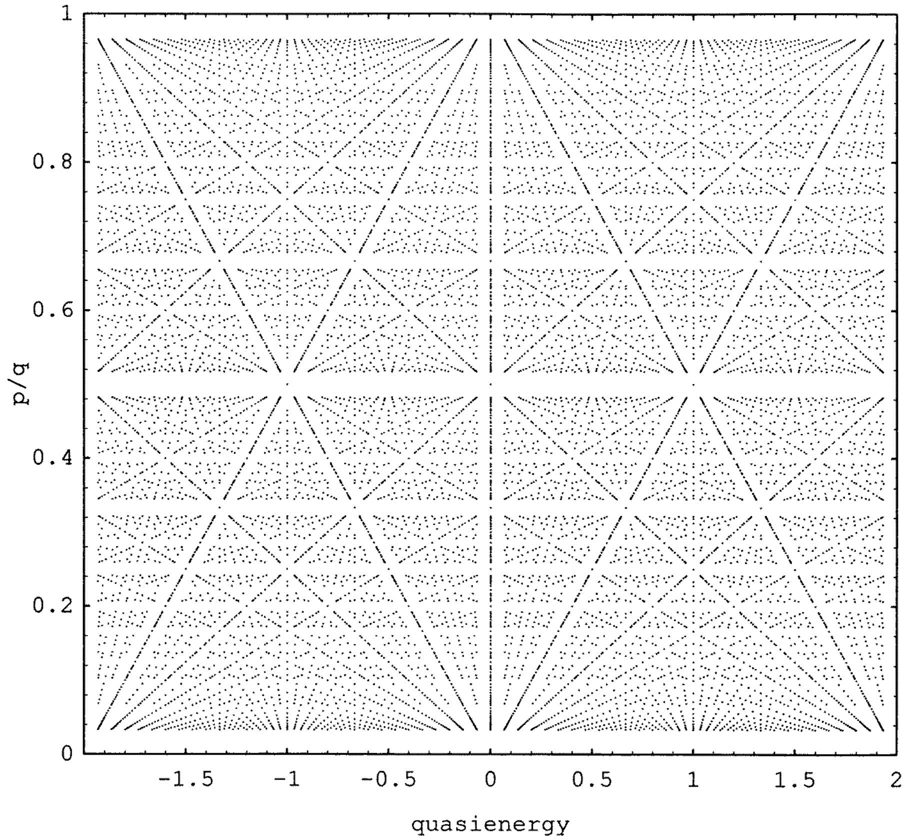

Figure 3. The quasi-energy versus the rational matching ratio, when $\alpha = n/(2n-1)$. The energies are in units of π/T and other parameters are arbitrary.

Stark ladders. For the lower curve, all resonant peaks but the Esaki–Tsu one have disappeared. This is just the manifestation of the total collapse of the quasi-energy bands.

4. Discussion and conclusions

We have solved analytically the problem of coherent motion of an electron in a one-dimensional long-period superlattice driven by a rectangular-wave electric field, of which both the dc and ac components can be adjusted simultaneously as the field parameters change. This system exhibits some distinctive features not encountered in the previously studied systems. The exact forms of the physical quantities such as the field-induced polarization, the mean square displacement, and the quasi-energy spectrum have been obtained explicitly. We found that when the matching ratio is rational, the electron can be localized even if we include long-range coupling terms, in contrast to the previously studied case. We also discovered the field condition at which the total collapse of the quasi-energy bands results and is manifested in I–V characteristic curves. In a laboratory set-up, this particular field is no more difficult to generate than a sinusoidal one. Thus it might be more conveniently used in manipulating the electrons in an energy band for the observation of the fractional Wannier–Stark ladders.

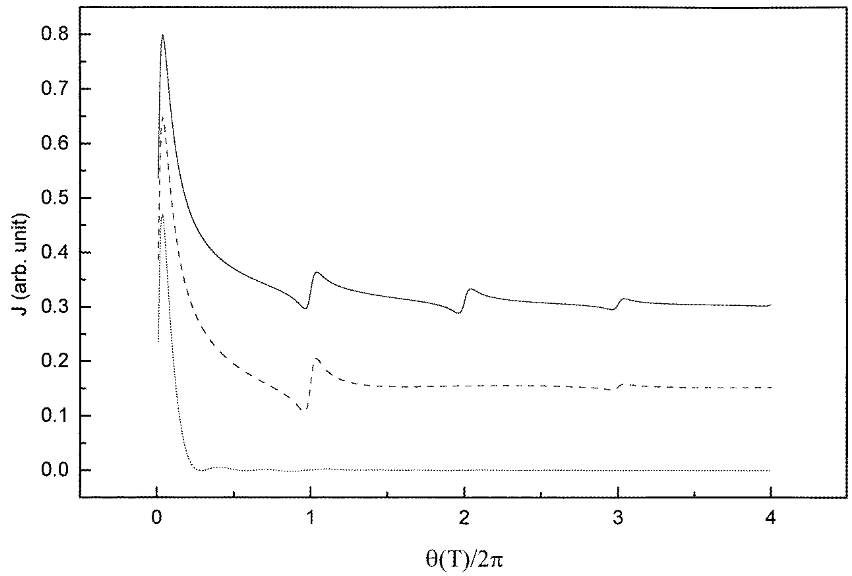

Figure 4. The I–V characteristic curves for $\alpha = 6/7$ (the upper curve), $3/4$ (the middle curve), and $4/7$ (the lower curve). To avoid overlaps, they have been shifted upwards by 0.3, 0.15, and 0.0, respectively. The relaxation time $\tau = 4T$.

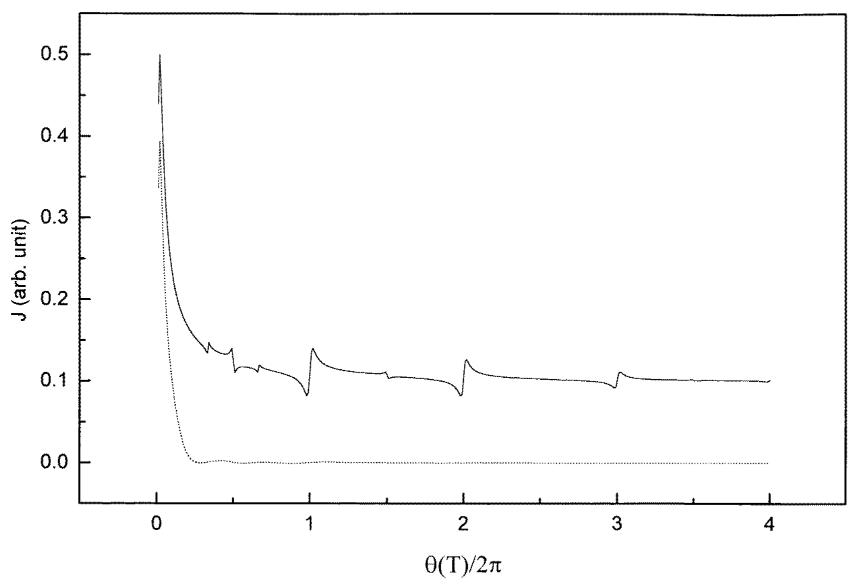

Figure 5. The I–V characteristic curves for $\alpha = 6/7$ (the upper curve) and $\alpha = 4/7$ (the lower curve). The upper curve has been shifted upwards by 0.1. The relaxation time $\tau = 10T$.

Acknowledgments

This work was supported in part by the National Natural Science Foundation of China under Grant No 19725417 and a grant from the China Academy of Engineering Physics. Q Niu gratefully acknowledges the support of the K C Wong Education Foundation, Hong Kong, and grants from the NSF and the R A Welch Foundation.

References

[1] Grifoni M and Hänggi P 1998 *Phys. Rep.* **304** 229
[2] Jauho A P and Johnsen K 1996 *Phys. Rev. Lett.* **76** 4576
[3] Wacker A, Jauho A P, Zeuner S and Allen S J 1998 *Phys. Rev.* B **56** 13 268
[4] Diez E, Gomez-Alcala R, Dominguez-Adame F, Sanchez A and Berman G P 1998 *Phys. Lett.* A **240** 109
[5] Wannier G H 1960 *Phys. Rev.* **117** 432
Wannier G H 1962 *Rev. Mod. Phys.* **34** 645
[6] Mendez E E, Agullo-Rueda F and Hong J M 1988 *Phys. Rev. Lett.* **60** 2426
Voisin P, Bleuse J, Bouche C, Gaillard S, Allibert C and Regreny A 1988 *Phys. Rev. Lett.* **61** 1639
[7] Niu Q, Zhao X-G, Georgakis G A and Raizen M G 1996 *Phys. Rev. Lett.* **76** 4504
[8] Ben Dahan M, Peik E, Reichel J, Castin Y and Salomon C 1996 *Phys. Rev. Lett.* **76** 4508
[9] Wilkinson S R, Bharucha C F, Madison K W, Niu Q and Raizen M G 1996 *Phys. Rev. Lett.* **76** 4512
[10] Dunlap D H and Kenkre V M 1986 *Phys. Rev.* B **34** 3625
Dunlap D H and Kenkre V M 1988 *Phys. Lett.* A **127** 438
[11] Holthaus M 1992 *Phys. Rev. Lett.* **69** 351
Zhao X-G 1994 *J. Phys.: Condens. Matter* **6** 2751
[12] Keay B J, Zeuner S, Allen S J, Maranowski K D, Gossard A C, Bhattacharya U and Rodwell M J W 1995 *Phys. Rev. Lett.* **75** 4102
[13] Zhao X-G 1991 *Phys. Lett.* A **155** 299
Zhao X-G 1992 *Phys. Lett.* A **167** 291
[14] Zhao X-G, Georgakis G A and Niu Q 1997 *Phys. Rev.* B **56** 3976
[15] Zhao X-G and Niu Q 1994 *Phys. Lett.* A **191** 181
[16] Avron J and Simon B 1982 *Bull. Am. Math. Soc.* **6** 81
Thouless D J and Niu Q 1983 *J. Phys. A: Math. Gen.* **16** 1911
[17] Zhao X-G, Jahnke R and Niu Q 1995 *Phys. Lett.* A **202** 297
[18] Bloch F 1928 *Z. Phys.* **52** 555
[19] Hofstadter D R 1976 *Phys. Rev.* B **14** 2239
[20] Niu Q 1989 *Phys. Rev.* B **40** 3625
[21] Esaki L and Tsu R 1970 *IBM J. Res. Dev.* **14** 61